Electronic Supplementary Material (ESI) for Physical Chemistry Chemical Physics

Theoretical Study of the Dynamic Electron-Spin-Polarization via Doublet-Quartet Quantum-Mixed State (II) – Population Transfer and Magnetic Field Dependence of the Spin Polarization -

Takafumi Matsumoto and Yoshio Teki*

Division of Molecular Material Science, Graduate School of Science,
Osaka City University
3-3-138 Sugimoto, Sumiyoshi-ku, Osaka 558-8585 (Japan)
E-mail: teki@sci.osaka-cu.ac.jp

Supplementary Information Data

The time-resolved ESR spectra and the details of the spectral simulations of **1** and **2**, the details of the spectral simulation using the eigenfield/exact-diagonalization hybrid method, the Spin Hamiltonian Matrix, the unitary transformation matrix from the W-basis to the S-basis representation, and projection operator P(D), the dynamic electron polarization density matrixes by the perturbation approach reported in our previous paper,[10] are presented as the supplementary information. The results of the non-coaxial case of $\boldsymbol{D}^{\mathrm{QM}}$ and $\boldsymbol{D}^{\mathrm{SC}}$ and the k/D^{QM} dependence on the population transfer in the case of small D^{QM} value are also presented.

(1) Time-Resolved ESR spectra and the details of the spectral simulations of 1 and 2.

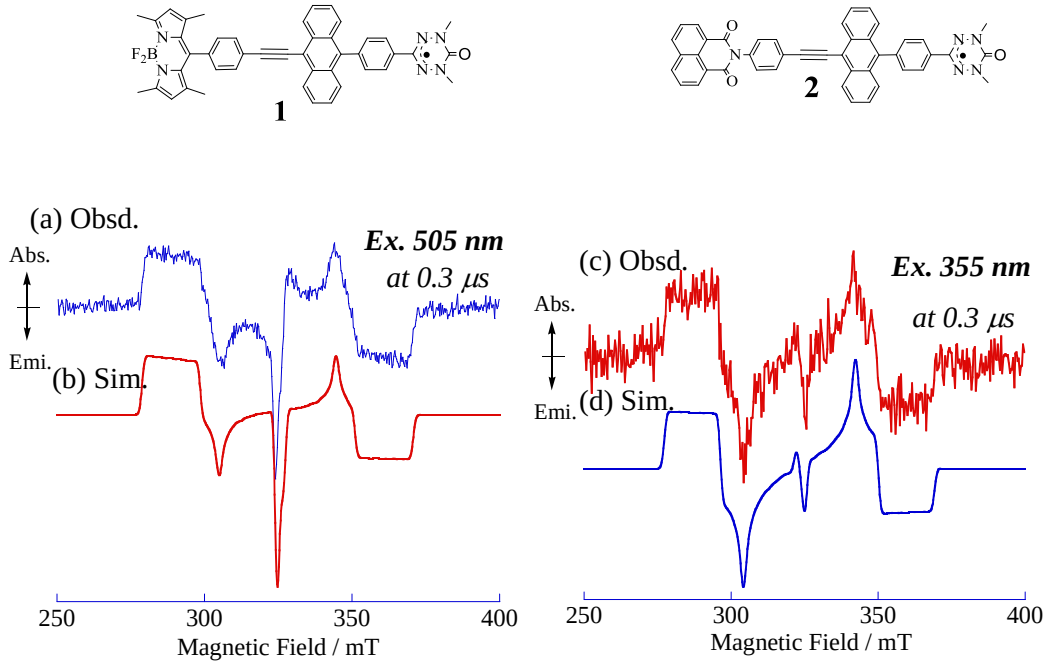

Figure S1 Observed time-resolved ESR spectrum of **1** and **2** and their spectral simulations reported in our previous papers.[11-13] (a) Observed TRESR spectrum of **1** after laser excitation of the absorption band (λ = 505 nm) of the bodipy component **A**; (b) Simulation obtained by the superimposition of the spectra of high-field DEP and zero-field DEP, and the polarized doublet with the weight of 0.45, 0.55, and 0.14, respectively.[11,12] ; (c) Observed TRESR spectrum of **2** obtained at 0.3 μs by the excitation of λ = 355 nm; (d) Simulation obtained by the superimposition of the spectra of high-field DEP and zero-field DEP, with the weight of 0.78 : 0.22, respectively. [13]

II) Spectral simulation using the eigenfield/exact-diagonalization hybrid method

The spectral simulations were carried out by exact numerical calculations, taking the DEP obtained above calculations into account. In the exact numerical spectral simulations, we used the eigenfield[45]/exact-diagonalization hybrid method.[46] The eigenfield/exact-diagonalization hybrid method[46] is a combination of the eigenfield method[45] (exact calculation of the ESR resonance fields) and the numerical diagonalization of the spin-Hamiltonian. In this method, the resonance field $B_{Res}(\theta, \phi)$ for each transition of $Ms \leftrightarrow Ms'$ was directly calculated by solving the following eigenfield equation:

$$A \bullet Z = B_{Res} C \bullet Z \quad , \qquad \text{(S1)}$$

where A and C are given by the following super-operators.

$$\boldsymbol{A} = \omega \boldsymbol{E} \otimes \boldsymbol{E} - \boldsymbol{F} \otimes \boldsymbol{E} + \boldsymbol{E} \otimes \boldsymbol{F} \qquad \text{(S2)}$$

and

$$\boldsymbol{C} = \boldsymbol{G} \otimes \boldsymbol{E} - \boldsymbol{E} \otimes \boldsymbol{G}^* \qquad \text{(S3)}$$

Here, $\boldsymbol{E}$ is a unit matrix and ω is the given microwave frequency. The operators $\boldsymbol{G}$ and $\boldsymbol{F}$ are the field dependent and independent parts of the spin Hamiltonian, respectively. By solving the eigenfield equation (eq (S1)), the resonance fields (B_{Res}) are obtained. The transition probabilities $I(\theta, \phi, \varphi)$ were evaluated by numerically diagonalization of the spin Hamiltonian matrix at each calculated resonance eigenfield. The line-shape function $S(B)$ of the time-resolved ESR spectrum in the glass matrix is given by

$$S(B) = N \sum \int_0^{\pi} d\varphi \int_0^{\pi} d\phi \int_0^{\pi} d\theta \sin\theta P_{Ms,Ms'}(\theta,\phi) I_{Ms,Ms'}(\theta,\phi,\varphi) f\,(B - B_{Ms,Ms'}(\theta,\phi)) \qquad (8)$$

In the simulation, $I_{Ms,\,Ms'}(\theta, \phi, \varphi)$ and $P_{Ms,\,Ms'}(\theta, \phi)$ are the transition probability which have been calculated by the exact numerical diagonalization of the spin Hamiltonian using the resonance fields and the deference of the populations (the diagonal terms of the density matrix, $\rho(t)$) between the M_S and the M_S' spin sublevels, respectively. Their populations of each spin-sublevels were calculated by the numerical solutions given by eq. (6) in the main text. A Gaussian type's line-shape function $f(B - B_{Ms,Ms'}(\theta,\phi))$ was used in the simulation.

III) Spin Hamiltonian Matrix, the unitary transformation matrix from the W-basis to the S-basis representation, and Projection Operator *P*(D)[10]

The spin Hamiltonian matrix of the QM state on the W basis representation is given by

$$H^{QM}=\begin{pmatrix} \omega_T+\omega_D/2 \\ -D_0^{QM}/2-J_W & \frac{1}{\sqrt{2}}(D_1^{QM})^* & \frac{1}{2}(D_2^{QM})^* & 0 & 0 & 0 \\ \frac{1}{\sqrt{2}}D_1^{QM} & \frac{1}{2}\omega_D+D_0^{QM} & -\frac{1}{\sqrt{2}}(D_1^{QM})^* & -\sqrt{2}J_W & 0 & 0 \\ \frac{1}{2}D_2^{QM} & -\frac{1}{\sqrt{2}}D_1^{QM} & \begin{matrix}-\omega_T+\omega_D/2 \\ -D_0^{QM}/2+J_W\end{matrix} & 0 & -\sqrt{2}J_W & 0 \\ 0 & -\sqrt{2}J_W & 0 & \begin{matrix}\omega_T-\omega_D/2 \\ -D_0^{QM}/2+J_W\end{matrix} & \frac{1}{\sqrt{2}}(D_1^{QM})^* & \frac{1}{2}(D_2^{QM})^* \\ 0 & 0 & -\sqrt{2}J_W & \frac{1}{\sqrt{2}}D_1^{QM} & -\frac{1}{2}\omega_D+D_0^{QM} & -\frac{1}{\sqrt{2}}(D_1^{QM})^* \\ 0 & 0 & 0 & \frac{1}{2}D_2^{QM} & -\frac{1}{\sqrt{2}}D_1^{QM} & \begin{matrix}-\omega_T-\omega_D/2 \\ -D_0^{QM}/2-J_W\end{matrix} \end{pmatrix}_W \quad (S4)$$

The unitary transformation matrix ($U^{W\to S}$) from the W basis representation to the S basis one (the unitary transformation diagonalizing H_{ex}) is obtained exactly using the Clebsch-Gordan coefficients.

$$U^{W\to S}=\begin{pmatrix} 1 & 0 & 0 & 0 & 0 & 0 \\ 0 & \sqrt{2/3} & 0 & 0 & -1/\sqrt{3} & 0 \\ 0 & 0 & 1/\sqrt{3} & 0 & 0 & -\sqrt{2/3} \\ 0 & 1/\sqrt{3} & 0 & 0 & \sqrt{2/3} & 0 \\ 0 & 0 & \sqrt{2/3} & 0 & 0 & 1/\sqrt{3} \\ 0 & 0 & 0 & 1 & 0 & 0 \end{pmatrix} \quad (S5)$$

The spin-Hamiltonian of the SC spin system: H^{SC} is given on the S basis representation by

$$H^{SC}=(U^{W\to S})^{-1}H^{QM}U^{W\to S}=\begin{pmatrix} H_Q & V_{DQ}^+ \\ V_{DQ} & H_D \end{pmatrix}_S , \quad \text{(S6a)}$$

where

$$H_Q=\begin{pmatrix} 3\omega_Q/2-3D_0^Q/2-J_S & \sqrt{3}(D_1^Q)^* & \sqrt{3}(D_2^Q)^*/2 & 0 \\ \sqrt{3}D_1^Q & \omega_Q/2+3D_0^Q/2-J_S & 0 & \sqrt{3}(D_2^Q)^*/2 \\ \sqrt{3}D_2^Q/2 & 0 & -\omega_Q/2+3D_0^Q/2-J_S & -\sqrt{3}(D_1^Q)^* \\ 0 & \sqrt{3}D_2^Q/2 & -\sqrt{3}D_1^Q & -3\omega_Q/2-3D_0^Q/2-J_S \end{pmatrix}_S \quad (S6b)$$

$$H_D=\begin{pmatrix} \omega_D/2+2J_S & 0 \\ 0 & -\omega_D/2+2J_S \end{pmatrix}_S \quad (S6c)$$

and

$$V_{DQ}=\begin{pmatrix} -\sqrt{3/2}D_1^Q & \sqrt{2}\Delta\omega_{DQ}/2-3\sqrt{2}D_0^Q/2 & 3\sqrt{2}(D_1^Q)^*/2 & \sqrt{3/2}(D_2^Q)^* \\ -\sqrt{3/2}D_2^Q & 3\sqrt{2}D_1^Q/2 & \sqrt{2}\Delta\omega_{DQ}/2+3\sqrt{2}D_0^Q/2 & -\sqrt{3/2}(D_1^Q)^* \end{pmatrix}_S . \quad \text{(S6d)}$$

Here, $g_Q = 2g^T(^TD^*)/3 + g^R/3$, $g_D = 4\,g^T(^TD^*)/3 - g^R/3$, $\boldsymbol{D}^Q = \boldsymbol{D}^T(^TD^*)/3$, $\omega_Q = g_Q\beta_e B$, $\omega_{DS} = g_D\beta_e B$, $\Delta g_{DQ} = g_D - g_Q = (2/3)(g^T(^TD^*) - g^R)$, and $\Delta\omega_{DQ} = \Delta g_{DQ}\beta_e B$. It is noted that H_Q and H_D are the spin Hamiltonians of the pure quartet state and the pure doublet state, respectively. The energy separation between their states is $3J_S$ and the mixing term V_{DQ} is negligible when $|J_S| >> |V_{DQ}|$, leading to the pure quartet and doublet states.

In the W basis representation, the projection operator $P(D)$ is given by

$$\hat{P}(D)=\begin{pmatrix} 0 & 0 & 0 & 0 & 0 & 0 \\ 0 & 1/6 & 0 & -\sqrt{2}/6 & 0 & 0 \\ 0 & 0 & 1/3 & 0 & -\sqrt{2}/6 & 0 \\ 0 & -\sqrt{2}/6 & 0 & 1/3 & 0 & 0 \\ 0 & 0 & -\sqrt{2}/6 & 0 & 1/6 & 0 \\ 0 & 0 & 0 & 0 & 0 & 0 \end{pmatrix}_W \qquad (S6e)$$

IV) Results of the perturbation approach reported in our previous paper[10]

We have treated the case of $|H_{ex}| < |H_f| << |H_z|$. Thus, $|H_f|$ and $|H_{ex}|$ were treated as perturbation terms. According to the conventional perturbation theory, the following equations have been derived.

Using a series of the unitary transformations, $\rho(t_3)_C^{\Psi}$ is obtained to the first order on the Ψ basis representation by

$$\begin{aligned}\rho(t_3)_C^{\Psi} &= (U^{S\to\Psi})^{-1}\rho(t_3)_C^{S}U^{S\to\Psi} \\ &= (U^{S\to\Psi})^{-1}(U^{W\to S})^{-1}(U^{\phi\to W})^{-1}\rho(t_2)_{DC}^{QM}U^{\phi\to W}U^{W\to S}U^{S\to\Psi}\end{aligned} \qquad \text{(S7)}$$

The de-coherence process leads to the selectively populated SC spin eigenstates which is represented on the Ψ basis representation.[10]

$$\rho(t_4)_{DC}^{\Psi}=\begin{pmatrix} 0 & 0 & 0 & 0 & 0 & 0 \\ 0 & \frac{2}{9}(1-\frac{2J_W}{\Delta_-})-\frac{\sqrt{2}\Omega_-}{27J_S} & 0 & 0 & 0 & 0 \\ 0 & 0 & \frac{2}{9}(1+\frac{2J_W}{\Delta_+})+\frac{\sqrt{2}\Omega_+}{27J_S} & 0 & 0 & 0 \\ 0 & 0 & 0 & 0 & 0 & 0 \\ 0 & 0 & 0 & 0 & \frac{5}{18}(1+\frac{8J_W}{5\Delta_-})+\frac{\sqrt{2}\Omega_-}{27J_S} & 0 \\ 0 & 0 & 0 & 0 & 0 & \frac{5}{18}(1-\frac{8J_W}{5\Delta_+})-\frac{\sqrt{2}\Omega_+}{27J_S} \end{pmatrix}_{\Psi} \qquad \text{(S8)}$$

V) D^{QM} Dependence on Population Transfer of the non-coaxial case of the fine-structure tensors, $\boldsymbol{D}^{\mathrm{QM}}$ and $\boldsymbol{D}^{\mathrm{SC}}$

Figure S2 shows that the dependence of the polarization transfer on the magnitude of D^{QM} value of the QM state in the several non-coaxial cases between $\boldsymbol{D}^{\mathrm{QM}}$ and $\boldsymbol{D}^{\mathrm{SC}}$ tensors. In the all calculations, E value of the tensor were assumed to be zero and the magnitude of D value was changed. The angle between the Euilar angle θ_1 of $\boldsymbol{D}^{\mathrm{QM}}$ and θ_2 of $\boldsymbol{D}^{\mathrm{SC}}$ were changed from 0 degree to 90 degree. k was set to be $1.0\mathrm{x}10^{7}$ s^{-1}, which is much slower than the Larmor procession. In this simulation, the detection time t was also set to be 1 s, because the population transfer from the QM state to the SC state was completed. The magnitude of D^{QM} values was varied. $2J_{\mathrm{W}}$ value was set to be a small value of $5.0\mathrm{x}10^{4}$ Hz (almost complete quantum-mixing condition). Other parameters were fixed as the same values used in the calculation of Figure 5 in the section I. Figure S3 shows that with becoming D^{QM}(Hz unit)/$k \cong 1$, the population transfer from the QM state to the SC quartet state started. With increasing D^{QM}(Hz unit)/k value, the populations of the SC quartet state increased. The polarization transfer occurs on the spin-sublevels with Ms $=\pm 1/2$ of the SC quartet state and the doublet state because of the Ms conservation during the polarization transfer. Interestingly, the magnitude of the D^{QM} value is just comparable to the Zeeman energy, anomaly on the polarization transfer is predicted as shown in Figure S2. These behaviors are almost same and not depend on the angle between θ_1 and θ_2. For the larger D^{QM} values, the polarization transfer depend on each spin-sublevels of the SC state and start to transfer to the spin-sublevels with Ms $= \pm 3/2$. The Ms conservation is broken in this region (large D^{QM} region). This may be owing to the quantized axes changing. As D^{QM}(Hz unit) much larger than the Zeeman frequency, the directions of the quantized axes become nearly parallel to the principal axes of the fine-structure tensor ($\boldsymbol{D}^{\mathrm{QM}}$) of the QM state. This leads to the constant values of the population of the spin-sublevels of the SC state. Only very slight dependence for the achieved constant values on the angle between θ_1 and θ_2 was observed as shown in this figure.

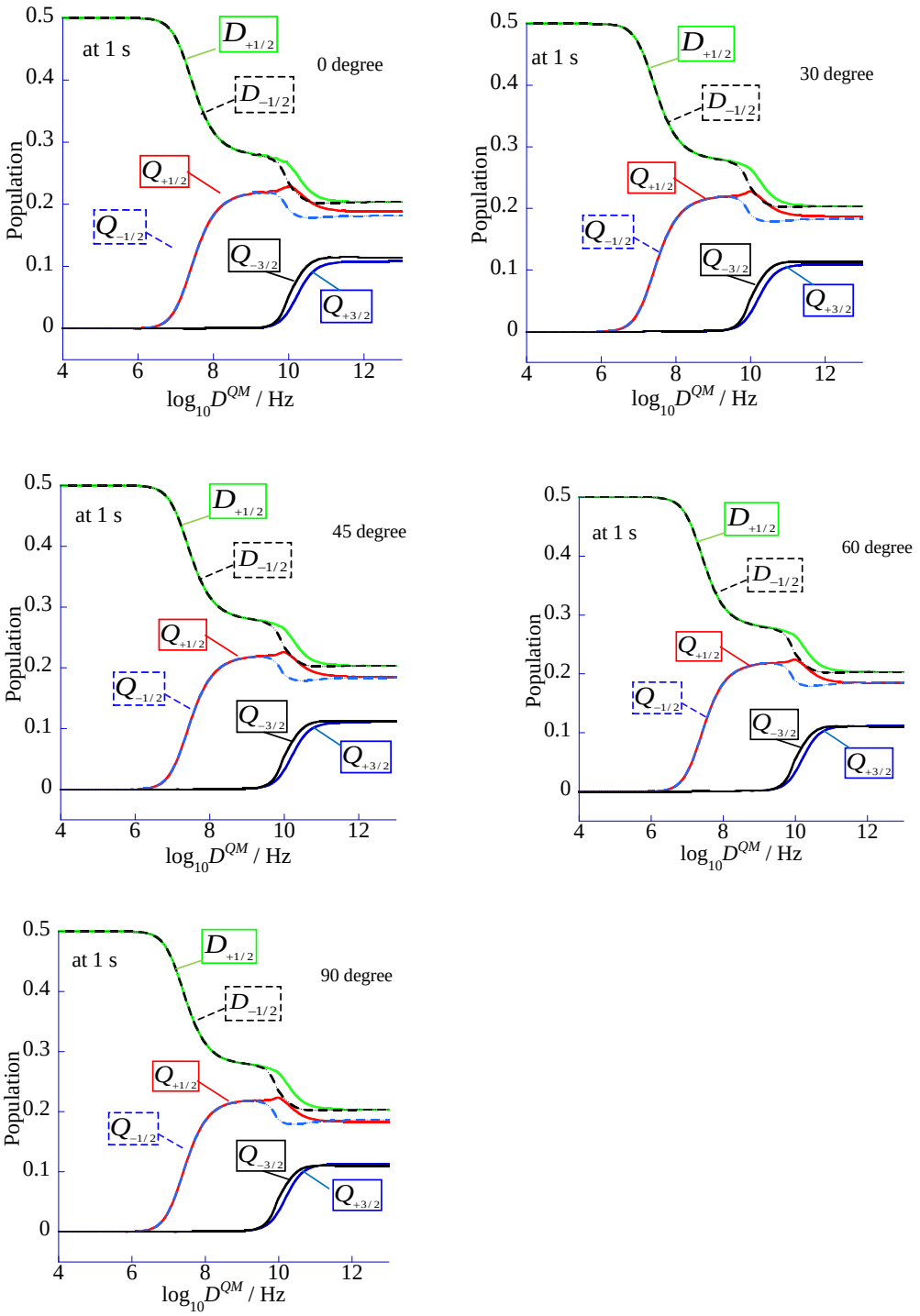

Figure S2 D^{QM} Dependence on Population Transfer of the non-coaxial case of the fine-structure tensors, D^{QM} and D^{SC}. The angle between θ_1 and θ_2 were changed from 0 degree to 90 degree. In order to remove the influence of the Δg effect, all g values (g^A, g^T g^R etc.) are set to be 2.0030.

VI) k/D^{QM} Dependence on Population Transfer in the Case of Small D^{QM} Value

When the magnitude of D^{QM} is close to the J_w value, a drastic change occurred, leading to the decrease to the population transfer to the SC quartet state. In the case of (a), the magnitude of D^{QM} (D^{QM}= 1x10^4 Hz) is smaller than the exchange interaction of the QM state ($2J_W$ = 5.0x10^4 Hz). There is no polarization trnsfer to the SC quartet state and the polarization transfer from the QM state occurs only to the SC doublet state. The decrease of the population appered in the region of k/D^{QM} < -3.5 comes from that the polarization transfer from the QM state to the SC state is not finished at the detection time, 1 s. In the case of (b), a small amount of the polarization is transferred to the SC quartet state in the reagion below $k/D^{QM} \cong 1$ ($\log_{10} k/D^{QM} \cong 0$). The decrease of the population appered in the region of k/D^{QM} < -4 comes from that the polarization transfer from the QM state to the SC state is not finished at the detection time, 1 s.

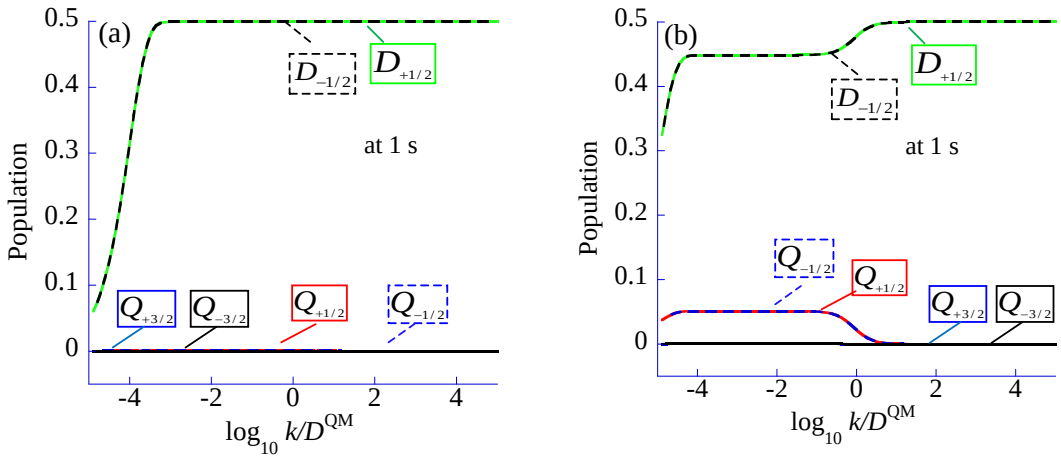

Figure S3 Dependence of the populations of each spin-sublevels of the SC state on the relative polarization transfer velocity k/D^{QM}. The spin Hamiltonian parameters used in this simulation are as follows. For the QM state, g^D = 2.0030, $g^T = g^T$ (**D**$^+$-**R**) = 2.0030, and $2J_W$ = 5.0x10^4 Hz. For the SC state, $g^D = g^R$ = 2.0030 and $g^T = g^T$ (^{T}**D***) = 2.0030, D^{SC} = 0.0645 cm^{-1}, E^{SC} = 0.0030 cm^{-1}, and $2J_S$ = 5.0x10^{12} Hz. E^{QM} = 0.0 Hz and $D^{QM}$was changed. (a) D^{QM}= 1x10^4 Hz, and (b) D^{QM}= 1x10^5 Hz in the frequency units. The k/D^{QM} ratio was chosen as the horizontal axis.